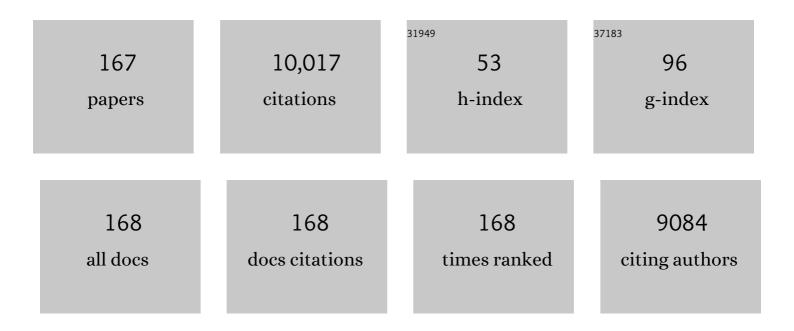
List of Publications by Year in descending order

Source: https://exaly.com/author-pdf/6423286/publications.pdf Version: 2024-02-01



VIIIMETIII

#	Article	IF	CITATIONS
1	Trace doping of multiple elements enables stable battery cycling of LiCoO2 at 4.6 V. Nature Energy, 2019, 4, 594-603.	19.8	572
2	Solar-driven, highly sustained splitting of seawater into hydrogen and oxygen fuels. Proceedings of the National Academy of Sciences of the United States of America, 2019, 116, 6624-6629.	3.3	524
3	In Operando X-ray Diffraction and Transmission X-ray Microscopy of Lithium Sulfur Batteries. Journal of the American Chemical Society, 2012, 134, 6337-6343.	6.6	475
4	Synchrotron X-ray Analytical Techniques for Studying Materials Electrochemistry in Rechargeable Batteries. Chemical Reviews, 2017, 117, 13123-13186.	23.0	390
5	Structure-Induced Reversible Anionic Redox Activity in Na Layered Oxide Cathode. Joule, 2018, 2, 125-140.	11.7	311
6	Oxygen Release Induced Chemomechanical Breakdown of Layered Cathode Materials. Nano Letters, 2018, 18, 3241-3249.	4.5	237
7	Three-dimensional imaging of chemical phase transformations at the nanoscale with full-field transmission X-ray microscopy. Journal of Synchrotron Radiation, 2011, 18, 773-781.	1.0	228
8	Highâ€Voltage Chargingâ€Induced Strain, Heterogeneity, and Microâ€Cracks in Secondary Particles of a Nickelâ€Rich Layered Cathode Material. Advanced Functional Materials, 2019, 29, 1900247.	7.8	219
9	<i>TXM-Wizard</i> : a program for advanced data collectionÂand evaluation in full-field transmission X-ray microscopy. Journal of Synchrotron Radiation, 2012, 19, 281-287.	1.0	217
10	Metal segregation in hierarchically structured cathode materials for high-energy lithiumÂbatteries. Nature Energy, 2016, 1, .	19.8	209
11	Low-dose, simple, and fast grating-based X-ray phase-contrast imaging. Proceedings of the National Academy of Sciences of the United States of America, 2010, 107, 13576-13581.	3.3	208
12	Enabling Stable Cycling of 4.2 V Highâ€Voltage Allâ€Solidâ€State Batteries with PEOâ€Based Solid Electrolyte. Advanced Functional Materials, 2020, 30, 1909392.	7.8	204
13	Quantification of Heterogeneous Degradation in Liâ€lon Batteries. Advanced Energy Materials, 2019, 9, 1900674.	10.2	176
14	Chemomechanical interplay of layered cathode materials undergoing fast charging in lithium batteries. Nano Energy, 2018, 53, 753-762.	8.2	173
15	Heterogeneous damage in Li-ion batteries: Experimental analysis and theoretical modeling. Journal of the Mechanics and Physics of Solids, 2019, 129, 160-183.	2.3	164
16	Nanoscale Morphological and Chemical Changes of High Voltage Lithium–Manganese Rich NMC Composite Cathodes with Cycling. Nano Letters, 2014, 14, 4334-4341.	4.5	163
17	In situ Visualization of State-of-Charge Heterogeneity within a LiCoO ₂ Particle that Evolves upon Cycling at Different Rates. ACS Energy Letters, 2017, 2, 1240-1245.	8.8	159
18	Charge Heterogeneity and Surface Chemistry in Polycrystalline Cathode Materials. Joule, 2018, 2, 464-477.	11.7	145

#	Article	IF	CITATIONS
19	Machine-learning-revealed statistics of the particle-carbon/binder detachment in lithium-ion battery cathodes. Nature Communications, 2020, 11, 2310.	5.8	143
20	Persistent Stateâ€ofâ€Charge Heterogeneity in Relaxed, Partially Charged Li _{1â^'} <i>_x</i> Ni _{1/3} Co _{1/3} Mn _{1/3} O ₂ Secondary Particles. Advanced Materials, 2016, 28, 6631-6638.	11.1	142
21	Chemomechanical behaviors of layered cathode materials in alkali metal ion batteries. Journal of Materials Chemistry A, 2018, 6, 21859-21884.	5.2	139
22	Additive engineering for robust interphases to stabilize high-Ni layered structures at ultra-high voltage of 4.8 V. Nature Energy, 2022, 7, 484-494.	19.8	138
23	Charge distribution guided by grain crystallographic orientations in polycrystalline battery materials. Nature Communications, 2020, 11, 83.	5.8	129
24	Life and death of a single catalytic cracking particle. Science Advances, 2015, 1, e1400199.	4.7	124
25	Phase transformation mechanism in lithium manganese nickel oxide revealed by single-crystal hard X-ray microscopy. Nature Communications, 2017, 8, 14309.	5.8	124
26	Depth-Dependent Redox Behavior of LiNi _{0.6} Mn _{0.2} Co _{0.2} O ₂ . Journal of the Electrochemical Society, 2018, 165, A696-A704.	1.3	123
27	Mesoscale Phase Distribution in Single Particles of LiFePO ₄ following Lithium Deintercalation. Chemistry of Materials, 2013, 25, 1664-1672.	3.2	120
28	Three-dimensional localization of nanoscale battery reactions using soft X-ray tomography. Nature Communications, 2018, 9, 921.	5.8	107
29	Formation of an interconnected network of iron melt at Earth's lower mantle conditions. Nature Geoscience, 2013, 6, 971-975.	5.4	106
30	Synergistically Enhancing the Therapeutic Effect of Radiation Therapy with Radiation Activatable and Reactive Oxygen Species-Releasing Nanostructures. ACS Nano, 2018, 12, 4946-4958.	7.3	101
31	Mapping Metals Incorporation of a Whole Single Catalyst Particle Using Element Specific X-ray Nanotomography. Journal of the American Chemical Society, 2015, 137, 102-105.	6.6	97
32	Hard Xâ€ray Nanotomography of Catalytic Solids at Work. Angewandte Chemie - International Edition, 2012, 51, 11986-11990.	7.2	96
33	Mesoscale Chemomechanical Interplay of the LiNi _{0.8} Co _{0.15} Al _{0.05} O ₂ Cathode in Solid-State Polymer Batteries. Chemistry of Materials, 2019, 31, 491-501.	3.2	89
34	Operando Revealing Dynamic Reconstruction of NiCo Carbonate Hydroxide for High-Rate Energy Storage. Joule, 2020, 4, 673-687.	11.7	88
35	Dynamics of particle network in composite battery cathodes. Science, 2022, 376, 517-521.	6.0	86
36	Ideal charge-density-wave order in the high-field state of superconducting YBCO. Proceedings of the National Academy of Sciences of the United States of America, 2016, 113, 14645-14650.	3.3	83

#	Article	IF	CITATIONS
37	Transmission Xâ€ray microscopy for fullâ€field nano imaging of biomaterials. Microscopy Research and Technique, 2011, 74, 671-681.	1.2	80
38	Understanding the Effect of Local Short-Range Ordering on Lithium Diffusion in Li1.3Nb0.3Mn0.4O2 Single-Crystal Cathode. CheM, 2018, 4, 2108-2123.	5.8	80
39	Nanoscale X-Ray Microscopic Imaging of Mammalian Mineralized Tissue. Microscopy and Microanalysis, 2010, 16, 327-336.	0.2	79
40	Mutual modulation between surface chemistry and bulk microstructure within secondary particles of nickel-rich layered oxides. Nature Communications, 2020, 11, 4433.	5.8	78
41	Relating structure and composition with accessibility of a single catalyst particle using correlative 3-dimensional micro-spectroscopy. Nature Communications, 2016, 7, 12634.	5.8	74
42	Hierarchical Defect Engineering for LiCoO2 through Low-Solubility Trace Element Doping. CheM, 2020, 6, 2759-2769.	5.8	74
43	Comparison of SOFC cathode microstructure quantified using X-ray nanotomography and focused ion beam–scanning electron microscopy. Electrochemistry Communications, 2011, 13, 586-589.	2.3	72
44	X-ray nanoscopy of cobalt Fischer–Tropsch catalysts at work. Chemical Communications, 2013, 49, 4622.	2.2	71
45	Stable Carbon–Selenium Bonds for Enhanced Performance in <i>Tremella</i> â€Like 2D Chalcogenide Battery Anode. Advanced Energy Materials, 2018, 8, 1800927.	10.2	68
46	3D elemental sensitive imaging using transmission X-ray microscopy. Analytical and Bioanalytical Chemistry, 2012, 404, 1297-1301.	1.9	63
47	Full-field XANES analysis of Roman ceramics to estimate firing conditions—A novel probe to study hierarchical heterogeneous materials. Journal of Analytical Atomic Spectrometry, 2013, 28, 1870.	1.6	63
48	Three-dimensional mapping of nickel oxidation states using full field x-ray absorption near edge structure nanotomography. Applied Physics Letters, 2011, 98, .	1.5	60
49	Nanoporous Tin with a Granular Hierarchical Ligament Morphology as a Highly Stable Li-Ion Battery Anode. ACS Applied Materials & Interfaces, 2017, 9, 293-303.	4.0	60
50	Propagation topography of redox phase transformations in heterogeneous layered oxide cathode materials. Nature Communications, 2018, 9, 2810.	5.8	59
51	Chemomechanics of Rechargeable Batteries: Status, Theories, and Perspectives. Chemical Reviews, 2022, 122, 13043-13107.	23.0	59
52	Mesoscale Battery Science: The Behavior of Electrode Particles Caught on a Multispectral X-ray Camera. Accounts of Chemical Research, 2018, 51, 2484-2492.	7.6	58
53	Highly active oxygen evolution integrated with efficient CO ₂ to CO electroreduction. Proceedings of the National Academy of Sciences of the United States of America, 2019, 116, 23915-23922.	3.3	58
54	Recent advances in synchrotron-based hard x-ray phase contrast imaging. Journal Physics D: Applied Physics, 2013, 46, 494001.	1.3	54

#	Article	IF	CITATIONS
55	Using X-ray Microscopy and Hg L ₃ XANES To Study Hg Binding in the Rhizosphere of <i>Spartina</i> Cordgrass. Environmental Science & Technology, 2009, 43, 7397-7402.	4.6	52
56	General 2.5 power law of metallic glasses. Proceedings of the National Academy of Sciences of the United States of America, 2016, 113, 1714-1718.	3.3	50
57	Surface-to-Bulk Redox Coupling through Thermally Driven Li Redistribution in Li- and Mn-Rich Layered Cathode Materials. Journal of the American Chemical Society, 2019, 141, 12079-12086.	6.6	47
58	A new iterative algorithm to reconstruct the refractive index. Physics in Medicine and Biology, 2007, 52, L5-L13.	1.6	46
59	Empowering multicomponent cathode materials for sodium ion batteries by exploring three-dimensional compositional heterogeneities. Energy and Environmental Science, 2018, 11, 2496-2508.	15.6	45
60	Thermal stress-induced charge and structure heterogeneity in emerging cathode materials. Materials Today, 2020, 35, 87-98.	8.3	45
61	Structural integrity—Searching the key factor to suppress the voltage fade of Li-rich layered cathode materials through 3D X-ray imaging and spectroscopy techniques. Nano Energy, 2016, 28, 164-171.	8.2	44
62	Operando Tailoring of Defects and Strains in Corrugated βâ€Ni(OH) ₂ Nanosheets for Stable and Highâ€Rate Energy Storage. Advanced Materials, 2021, 33, e2006147.	11.1	44
63	Nonequilibrium Pathways during Electrochemical Phase Transformations in Single Crystals Revealed by Dynamic Chemical Imaging at Nanoscale Resolution. Advanced Energy Materials, 2015, 5, 1402040.	10.2	42
64	Finding a Needle in the Haystack: Identification of Functionally Important Minority Phases in an Operating Battery. Nano Letters, 2017, 17, 7782-7788.	4.5	42
65	Understanding the Mesoscale Degradation in Nickel-Rich Cathode Materials through Machine-Learning-Revealed Strain–Redox Decoupling. ACS Energy Letters, 2021, 6, 687-693.	8.8	42
66	Selective dopant segregation modulates mesoscale reaction kinetics in layered transition metal oxide. Nano Energy, 2021, 84, 105926.	8.2	42
67	Phase retrieval in x-ray imaging based on using structured illumination. Physical Review A, 2008, 78, .	1.0	41
68	Thermally-driven mesopore formation and oxygen release in delithiated NCA cathode particles. Journal of Materials Chemistry A, 2019, 7, 12593-12603.	5.2	41
69	Evolution of Local Structural Ordering and Chemical Distribution upon Delithiation of a Rock Salt–Structured Li _{1.3} Ta _{0.3} Mn _{0.4} O ₂ Cathode. Advanced Functional Materials, 2019, 29, 1808294.	7.8	41
70	Phase retrieval using polychromatic illumination for transmission X-ray microscopy. Optics Express, 2011, 19, 540.	1.7	40
71	Thermally driven mesoscale chemomechanical interplay in Li _{0.5} Ni _{0.6} Mn _{0.2} Co _{0.2} O ₂ cathode materials. Journal of Materials Chemistry A, 2018, 6, 23055-23061.	5.2	38
72	To get the most out of high resolution X-ray tomography: A review of the post-reconstruction analysis. Spectrochimica Acta, Part B: Atomic Spectroscopy, 2016, 117, 29-41.	1.5	37

#	Article	IF	CITATIONS
73	Computational Modeling of Heterogeneity of Stress, Charge, and Cyclic Damage in Composite Electrodes of Li-Ion Batteries. Journal of the Electrochemical Society, 2020, 167, 040527.	1.3	36
74	Temperature-Swing Synthesis of Large-Size Single-Crystal LiNi _{0.6} Mn _{0.2} Co _{0.2} O ₂ Cathode Materials. Journal of the Electrochemical Society, 2021, 168, 010534.	1.3	36
75	Utilizing Environmental Friendly Iron as a Substitution Element in Spinel Structured Cathode Materials for Safer High Energy Lithiumâ€ion Batteries. Advanced Energy Materials, 2016, 6, 1501662.	10.2	35
76	Depth-dependent valence stratification driven by oxygen redox in lithium-rich layered oxide. Nature Communications, 2020, 11, 6342.	5.8	34
77	Extended depth of focus for transmission x-ray microscope. Optics Letters, 2012, 37, 3708.	1.7	33
78	3D Nanoscale Chemical Imaging of the Distribution of Aluminum Coordination Environments in Zeolites with Soft Xâ€Ray Microscopy. ChemPhysChem, 2013, 14, 496-499.	1.0	33
79	Thermal-healing of lattice defects for high-energy single-crystalline battery cathodes. Nature Communications, 2022, 13, 704.	5.8	33
80	The role of structural defects in commercial lithium-ion batteries. Cell Reports Physical Science, 2021, 2, 100554.	2.8	32
81	Structural, Dynamic, and Chemical Complexities in Zinc Anode of an Operating Aqueous Znâ€lon Battery. Advanced Energy Materials, 2022, 12, .	10.2	32
82	Diffraction enhanced imaging: a simple model. Journal Physics D: Applied Physics, 2006, 39, 4142-4147.	1.3	31
83	Characterization of heterogeneity in the Heletz sandstone from core to pore scale and quantification of its impact on multi-phase flow. International Journal of Greenhouse Gas Control, 2016, 48, 69-83.	2.3	31
84	Applications of Hard Xâ€ray Fullâ€Field Transmission Xâ€ray Microscopy at SSRL. AlP Conference Proceedings, 2011, , .	0.3	29
85	Study on the synthesis–microstructure-performance relationship of layered Li-excess nickel–manganese oxide as a Li-ion battery cathode prepared by high-temperature calcination. Journal of Materials Chemistry A, 2013, 1, 10847.	5.2	29
86	Multiphase, Multiscale Chemomechanics at Extreme Low Temperatures: Battery Electrodes for Operation in a Wide Temperature Range. Advanced Energy Materials, 2021, 11, 2102122.	10.2	27
87	Structural and chemical evolution in layered oxide cathodes of lithium-ion batteries revealed by synchrotron techniques. National Science Review, 2022, 9, nwab146.	4.6	27
88	Heterogeneous Reaction Activities and Statistical Characteristics of Particle Cracking in Battery Electrodes. ACS Energy Letters, 2021, 6, 4065-4070.	8.8	26
89	Value-creating upcycling of retired electric vehicle battery cathodes. Cell Reports Physical Science, 2022, 3, 100741.	2.8	24
90	Unsupervised Data Mining in nanoscale X-ray Spectro-Microscopic Study of NdFeB Magnet. Scientific Reports, 2016, 6, 34406.	1.6	23

#	Article	IF	CITATIONS
91	Automatic projection image registration for nanoscale X-ray tomographic reconstruction. Journal of Synchrotron Radiation, 2018, 25, 1819-1826.	1.0	23
92	High pressure nano-tomography using an iterative method. Journal of Applied Physics, 2012, 111, 112626.	1.1	22
93	Nanoscale elemental sensitivity study of Nd ₂ Fe ₁₄ B using absorption correlation tomography. Microscopy Research and Technique, 2013, 76, 1112-1117.	1.2	22
94	Evolution of the nanoporous microstructure of sintered Ag at high temperature using in-situ X-ray nanotomography. Acta Materialia, 2018, 156, 310-317.	3.8	22
95	Uncovering phase transformation, morphological evolution, and nanoscale color heterogeneity in tungsten oxide electrochromic materials. Journal of Materials Chemistry A, 2020, 8, 20000-20010.	5.2	21
96	Extraction of pore-morphology and capillary pressure curves of porous media from synchrotron-based tomography data. Scientific Reports, 2015, 5, 10635.	1.6	20
97	Ultrafast Construction of Oxygen-Containing Scaffold over Graphite for Trapping Ni ²⁺ into Single Atom Catalysts. ACS Nano, 2020, 14, 11662-11669.	7.3	20
98	Registration of the rotation axis in X-ray tomography. Journal of Synchrotron Radiation, 2015, 22, 452-457.	1.0	19
99	Sodium Ion Batteries: Stable Carbon–Selenium Bonds for Enhanced Performance in <i>Tremella</i> â€Like 2D Chalcogenide Battery Anode (Adv. Energy Mater. 23/2018). Advanced Energy Materials, 2018, 8, 1870106.	10.2	19
100	Distinct Surface and Bulk Thermal Behaviors of LiNi _{0.6} Mn _{0.2} Co _{0.2} O ₂ Cathode Materials as a Function of State of Charge. ACS Applied Materials & Interfaces, 2020, 12, 11643-11656.	4.0	19
101	Fast Li Plating Behavior Probed by X-ray Computed Tomography. Nano Letters, 2021, 21, 5254-5261.	4.5	19
102	Anomalous Thermal Decomposition Behavior of Polycrystalline LiNi _{0.8} Mn _{0.1} Co _{0.1} O ₂ in PEOâ€Based Solid Polymer Electrolyte. Advanced Functional Materials, 2022, 32, .	7.8	19
103	Full-field transmission x-ray microscopy for bio-imaging. Journal of Physics: Conference Series, 2009, 186, 012081.	0.3	18
104	Five-dimensional visualization of phase transition in BiNiO3 under high pressure. Applied Physics Letters, 2014, 104, 043108.	1.5	18
105	High-resolution multicontrast tomography with an X-ray microarray anode–structured target source. Proceedings of the National Academy of Sciences of the United States of America, 2021, 118, .	3.3	18
106	A Hierarchical-Structured Impeller with Engineered Pd Nanoparticles Catalyzing Suzuki Coupling Reactions for High-Purity Biphenyl. ACS Applied Materials & Interfaces, 2021, 13, 17429-17438.	4.0	16
107	Reversible Mn/Cr dual redox in cation-disordered Li-excess cathode materials for stable lithium ion batteries. Acta Materialia, 2021, 212, 116935.	3.8	16
108	Evidence for oxygenation of Fe-Mg oxides at mid-mantle conditions and the rise of deep oxygen. National Science Review, 2021, 8, nwaa096.	4.6	15

#	Article	IF	CITATIONS
109	Understanding multi-scale battery degradation with a macro-to-nano zoom through its hierarchy. Journal of Materials Chemistry A, 2021, 9, 19886-19893.	5.2	14
110	Machine-and-data intelligence for synchrotron science. Nature Reviews Physics, 2021, 3, 766-768.	11.9	14
111	Surface Characterization of Li-Substituted Compositionally Heterogeneous NaLi _{0.045} Cu _{0.185} Fe _{0.265} Mn _{0.505} O ₂ Sodium-Ion Cathode Material. Journal of Physical Chemistry C, 2019, 123, 11428-11435.	1.5	13
112	High-dimensional and high-resolution x-ray tomography for energy materials science. MRS Bulletin, 2020, 45, 283-289.	1.7	13
113	Three-dimensional microstructural mapping of poisoning phases in the Neodymium Nickelate solid oxide fuel cell cathode. Solid State Ionics, 2013, 237, 16-21.	1.3	12
114	Quantifying redox heterogeneity in single-crystalline LiCoO ₂ cathode particles. Journal of Synchrotron Radiation, 2020, 27, 713-719.	1.0	12
115	Applications for Nanoscale X-ray Imaging at High Pressure. Engineering, 2019, 5, 479-489.	3.2	11
116	Automatic 3D image registration for nano-resolution chemical mapping using synchrotron spectro-tomography. Journal of Synchrotron Radiation, 2021, 28, 278-282.	1.0	11
117	Nanoscale Visualization of Gas Shale Pore and Textural Features. , 2013, , .		10
118	Tracerâ€Guided Characterization of Dominant Pore Networks and Implications for Permeability and Wettability in Shale. Journal of Geophysical Research: Solid Earth, 2019, 124, 1459-1479.	1.4	10
119	Investigating Particle Sizeâ€Dependent Redox Kinetics and Charge Distribution in Disordered Rocksalt Cathodes. Advanced Functional Materials, 2022, 32, .	7.8	10
120	Deep-learning-based image registration for nano-resolution tomographic reconstruction. Journal of Synchrotron Radiation, 2021, 28, 1909-1915.	1.0	9
121	Deepâ€Learningâ€Enabled Crack Detection and Analysis in Commercial Lithiumâ€Ion Battery Cathodes. Advanced Functional Materials, 2022, 32, .	7.8	9
122	Direct observation of the kinetics of gas–solid reactions using <i>in situ</i> kinetic and spectroscopic techniques. Reaction Chemistry and Engineering, 2018, 3, 668-675.	1.9	8
123	Role of Fluorine in Chemomechanics of Cation-Disordered Rocksalt Cathodes. Chemistry of Materials, 2021, 33, 7028-7038.	3.2	8
124	In Situ Visualization of Li-Whisker with Grating-Interferometry-Based Tricontrast X-ray Microtomography. , 2021, 3, 1786-1792.		8
125	Phase retrieval from a single near-field diffraction pattern with a large Fresnel number. Journal of the Optical Society of America A: Optics and Image Science, and Vision, 2008, 25, 2651.	0.8	7
126	Analysis of partial coherence in grating-based phase-contrast X-ray imaging. Nuclear Instruments and Methods in Physics Research, Section A: Accelerators, Spectrometers, Detectors and Associated Equipment, 2010, 619, 319-322.	0.7	7

#	Article	IF	CITATIONS
127	Imaging translocation and transformation of bioavailable selenium by Stanleya pinnata with X-ray microscopy. Analytical and Bioanalytical Chemistry, 2012, 404, 1277-1285.	1.9	7
128	Transformations and Decomposition of MnCO3 at Earth's Lower Mantle Conditions. Frontiers in Earth Science, 2016, 4, .	0.8	7
129	Elemental and Chemical Mapping of High Capacity Intermetallic Li-ion Anodes with Transmission X-ray Microscopy. Jom, 2017, 69, 1478-1483.	0.9	7
130	A Study of Modelâ€Based Protective Fastâ€Charging and Associated Degradation in Commercial Smartphone Cells: Insights on Cathode Degradation as a Result of Lithium Depositions on the Anode. Advanced Energy Materials, 2021, 11, 2003019.	10.2	7
131	Probing lattice defects in crystalline battery cathode using hard X-ray nanoprobe with data-driven modeling. Energy Storage Materials, 2022, 45, 647-655.	9.5	7
132	Resolving Charge Distribution for Compositionally Heterogeneous Battery Cathode Materials. Nano Letters, 2022, 22, 1278-1286.	4.5	7
133	Comparative analysis of phase extraction methods based on phase-stepping and shifting curve in grating interferometry. Chinese Physics B, 2010, 19, 040701.	0.7	6
134	Comparison of X-ray Nanotomography and FIB-SEM in Quantifying the Composite LSM/YSZ SOFC Cathode Microstructure. ECS Transactions, 2011, 35, 2417-2421.	0.3	6
135	Threeâ€dimensional mapping of crystalline ceramic waste form materials. Journal of the American Ceramic Society, 2017, 100, 3722-3735.	1.9	6
136	Quantitative probing of the fast particle motion during the solidification of battery electrodes. Applied Physics Letters, 2020, 116, .	1.5	6
137	In situ visualization of multicomponents coevolution in a battery pouch cell. Proceedings of the National Academy of Sciences of the United States of America, 2022, 119, .	3.3	6
138	Data-Driven Lithium-Ion Battery Cathode Research with State-of-the-Art Synchrotron X-ray Techniques. Accounts of Materials Research, 2022, 3, 854-865.	5.9	6
139	Investigation of misalignment in analyzer crystal based-CT and its effect. Physics in Medicine and Biology, 2008, 53, 5757-5766.	1.6	5
140	Investigation of biomedical inner microstructures with hard X-ray phase-contrast imaging. Nuclear Instruments and Methods in Physics Research, Section A: Accelerators, Spectrometers, Detectors and Associated Equipment, 2007, 580, 610-613.	0.7	4
141	Theory and experiment of in-line phase contrast imaging on non-uniformly distributed source. Spectrochimica Acta, Part B: Atomic Spectroscopy, 2007, 62, 636-641.	1.5	4
142	Fresnel zone-plate based X-ray microscopy in Zernike phase contrast with sub-50 nm resolution at NSRL. Journal of Physics: Conference Series, 2009, 186, 012005.	0.3	4
143	Monitoring Deformation in Graphene Through Hyperspectral Synchrotron Spectroscopy to Inform Fabrication. Journal of Physical Chemistry C, 2017, 121, 15653-15664.	1.5	3
144	Characterization of photoinduced normal state through charge density wave in superconducting YBa ₂ Cu ₃ O _{6.67} . Science Advances, 2022, 8, eabk0832.	4.7	3

#	Article	IF	CITATIONS
145	Principle of diffraction enhanced imaging (DEI) and computed tomography based on DEI method. Nuclear Science and Techniques/Hewuli, 2006, 17, 342-353.	1.3	2
146	Image enhancement of x-ray microscope using frequency spectrum analysis. Journal of Physics: Conference Series, 2009, 186, 012009.	0.3	2
147	Synchrotron-based transmission x-ray microscopy for improved extraction in shale during hydraulic fracturing. Proceedings of SPIE, 2015, , .	0.8	2
148	Understanding spin configuration in the geometrically frustrated magnet TbB4: A resonant soft X-ray scattering study. Current Applied Physics, 2018, 18, 1205-1211.	1.1	2
149	In-Situ Visualization of the Transition Metal Dissolution in Layered Cathodes. Journal of Electrochemical Energy Conversion and Storage, 2022, 19, .	1.1	2
150	Edge enhanced X-ray phase tomography. Nuclear Instruments and Methods in Physics Research, Section A: Accelerators, Spectrometers, Detectors and Associated Equipment, 2007, 580, 617-620.	0.7	1
151	Full Field Imaging of Nickel Oxidation States in Solid Oxide Fuel Cell Anode Materials by Xanes Nanotomography. , 2011, , .		1
152	3D Imaging of Nickel Oxidation States using Full Field X-ray Absorption Near Edge Structure Nanotomography. ECS Transactions, 2011, 35, 1315-1321.	0.3	1
153	Data-processing strategies for nano-tomography with elemental specification. Proceedings of SPIE, 2013, , .	0.8	1
154	Applications of Full-field Transmission X-ray Nanotomography and X-ray Nanospectroscopy at Stanford Synchrotron Radiation Lightsource. Microscopy and Microanalysis, 2020, 26, 778-780.	0.2	1
155	Experimental and theoretical investigations of diffraction enhanced imaging. Nuclear Instruments and Methods in Physics Research, Section A: Accelerators, Spectrometers, Detectors and Associated Equipment, 2007, 580, 803-807.	0.7	0
156	Analysis of Solid Oxide Fuel Cell LSM-YSZ Composite Cathodes With Varying Starting Powder Sizes. , 2011, , .		0
157	SSRL/LCLS Users' Meeting and Workshops Draw Hundreds to SLAC. Synchrotron Radiation News, 2014, 27, 49-55.	0.2	0
158	Sub-100 nm resolution 3-D tomography of CZTSe using transmission X-ray Microscopy. , 2015, , .		0
159	Cu 2 ZnSnSe 4 Photovoltaic Absorber Layers Evaluated by Transmission Xâ€Ray Microscopy Tomography: Composition Fluctuations on the Length Scale of Grains. Solar Rrl, 2017, 1, 1600024.	3.1	0
160	Synchrotron Radiation Nanoscale X-ray Imaging Technology And Scientific Big Data Mining Assist Energy Materials Research. Microscopy and Microanalysis, 2018, 24, 542-543.	0.2	0
161	Simultaneous threeâ€dimensional elemental mapping of Hollandite and Pyrochlore material phases in ceramic waste form materials. Journal of the American Ceramic Society, 2019, 102, 5620-5631.	1.9	0
162	(Invited) Hierarchical Defect Engineering for Electrochemical Energy Storage Materials. ECS Meeting Abstracts, 2021, MA2021-01, 1976-1976.	0.0	0

#	Article	IF	CITATIONS
163	The interplay among compositional heterogeneity, lattice defects, micromorphology, and redox stratification in lithium-ion batteries. Microscopy and Microanalysis, 2021, 27, 1216-1217.	0.2	0
164	(Invited) Dynamic Plating/Stripping Behavior of Zn Anode in an Operating Aqueous Zn-Ion Battery. ECS Meeting Abstracts, 2022, MA2022-01, 1192-1192.	0.0	0
165	Heterogeneous Damage and Network Evolution in Composite Electrodes of Li-Ion Batteries. ECS Meeting Abstracts, 2022, MA2022-01, 1637-1637.	0.0	Ο
166	(Invited) Mesoscale Reaction Kinetics Modulated By Structural and Compositional Heterogeneity in Battery Cathode Materials. ECS Meeting Abstracts, 2022, MA2022-01, 1635-1635.	0.0	0
167	(Invited) A Macro-to-Nano Zoom through the Hierarchy of a Lithium Ion Battery. ECS Meeting Abstracts, 2022, MA2022-01, 1650-1650.	0.0	0